

Experimental testing and modelling of an industrial insulated pipeline for deep sea application

Nadège Bouchonneau^{a, b, c, *}, Valérie Sauvart-Moynot^{a, 1}, Dominique Choqueuse^{b, 2}, François Grosjean^{a, 1}, Emmanuel Poncet^{c, 3} and Dominique Perreux^{c, 3}

^a IFP Lyon, Département Chimie et Physico-Chimie Appliquées, 69360 Solaize, France

^b Institut Français de Recherche pour l'Exploitation de la Mer (IFREMER), Service Matériaux et Structures, 29280 Plouzané, France

^c Université de Franche-Comté, FEMTO-ST, 25000 Besançon, France

*: Corresponding author : N. Bouchonneau, Tel.: + 33 4 78 02 26 85, + 33 2 98 22 41 63, + 33 3 81 66 60 12; fax: + 33 4 78 02 21 41, + 33 2 98 22 45 35, + 33 3 81 66 67 00, email address : nadege.bouchonneau@gmail.com

¹ Tel.: + 33 4 78 02 26 85; fax: + 33 4 78 02 21 41.

² Tel.: + 33 2 98 22 41 63; fax: + 33 2 98 22 45 35.

³ Tel.: + 33 3 81 66 60 12; fax: + 33 3 81 66 67 00.

Abstract:

Ultra-deep water (up to 3000 m) is one of the next frontiers for oil offshore exploitation. It requires the use of conduits having to resist in the long run (durability about 25 years) the mechanical and environmental requests. One of the key points is the thermal insulation of the structure to avoid the formation of hydrates and paraffin plugs inside of the steel pipe. Over the past 10 years, many studies were performed to better understand the behaviour of the syntactic foams used as thermal insulation of pipes for deepwater production, but few tests were run on industrial prototypes to reach the actual thermal properties of the systems.

This paper presents the numerical and experimental characterizations of an industrial multilayered insulated pipeline tested in service conditions. Two thermomechanical finite element modellings of the coated pipeline have been developed to predict its behaviour during service condition tests. The first model considers pure conduction through the inner air inside of the structure and the second model considers convection phenomenon between the inner air and the metallic surfaces inside of the structure. In parallel, industrial pipe tests on an immersed instrumented pipeline, internally heated to temperatures up to 95 °C and subjected externally to hydrostatic pressure up to 300 bar are presented. Experimental data obtained during industrial pipe tests and related model predictions are compared and discussed. Thermal properties of the syntactic foam are determined with steady and transient states analysis. In complement, a study of the model results sensitivity to the input Poisson coefficient is presented.

Keywords: layered structure; subsea; thermal properties; modelling; syntactic foam

Nomenclature

a	thermal diffusivity [$\text{m}^2 \text{s}^{-1}$].
D_i	inner diameter of the layer i of the structure [m].
D_{i+1}	external diameter of the layer i of the structure [m].
D_1	inner diameter of the steel pipe [m].
h_{ext}	convective heat transfer coefficient at the interface between insulation coating and water [$\text{W m}^{-2} \text{K}^{-1}$].
L	steel pipe length [m].
λ_i	thermal conductivity of the layer i [$\text{W m}^{-1} \text{K}^{-1}$].
S	inner surface area, expressed as $S = \pi L D_1$ [m^2].
S_{ext}	external surface area [m^2].
T	temperature [K].
T_0	initial temperature [$^{\circ}\text{C}$].
T_{ext}	external surface temperature in steady state conditions [$^{\circ}\text{C}$].
T_{int}	internal surface temperature in steady state conditions [$^{\circ}\text{C}$].
U	global heat transfer coefficient of the structure relative to a reference surface [$\text{W m}^{-2} \text{K}^{-1}$].

1. Introduction

Since new hydrocarbon reserves discoveries are more and more rare in the conventional offshore, the industry is looking into new hydrocarbon reserves perspectives located in deep sea (between 500 and 1 500 m) and ultra-deep sea (between 1 500 and 3 000 m) as underlined by Robertson et al. (2005). Thus, one of the currently most challenging projects in the petroleum industry consists of exploiting oil resources at great depths, where production infrastructures are submitted to high hydrostatic pressures (up to 300bar) and to low external temperatures (about 4 °C at 3000 m). To limit heat losses and so avoid the formation of hydrate and wax plugs inside subsea production flowlines or risers under such pressure and temperature conditions, even during production shutdowns, the pipelines need to be thermally insulated. One of the most efficient type of thermal insulation systems is the multilayered structure made of several materials of different thicknesses directly applied to the external surface of the steel pipe. Currently used materials in thermal insulated multilayered systems for deep sea applications include massive polymers and syntactic foams, composed of hollow glass microspheres embedded in a polymer matrix. These composites must combine thermal insulation function, low buoyancy while providing good compressive strength.

To date, most of the studies conducted in this domain were performed on small samples in order to evaluate material performance under representative conditions of pressure, temperature and ageing media, as studied by Choqueuse et al. (2002), (2003), (2005) and Gimenez et al. (2005). Up to now, just few experimental recent studies deal with thermal performance evaluation on large-scale multilayered insulated pipelines submitted to severe conditions. Such upscale structure tests were performed by Haldane et al. (1999), (2001) in the Heriot-Watt and TNO Institute of Applied Physics work, who developed a direct measurement system to determine in-situ the thermal characteristics of insulated pipes submitted to hydrostatic pressures up to 145 bar, internally heated with circulating oil (up to 140 °C) and with external cooling at 8 °C.

With the development of ultra-deep offshore fields high hydrostatic loads are reached which could have drastic consequences on the insulation coating performance. In this paper, experimental tests on an industrial pipe under higher hydrostatic pressures (up to 300bar) have been developed and performed in order to study the multilayered structure thermal performances in ultra-deep service conditions. The results obtained with two tested prototypes have previously been compared to validate the experimental protocol by Bouchonneau et al. (2007).

A thermomechanical modelling of multilayered structures in simulated severe service conditions, based on experimental data collected on samples, is presented. In fact, two hypotheses (internal conduction and internal convection) are presented and compared. These numerical models were developed in order to predict the thermomechanical behaviour of a complex industrial structure composed of different materials.

In parallel, tests on industrial structure up to 300bar hydrostatic pressure (simulating ultra-deep water) have been conducted to study the influence of high pressure loads on thermal performances of the syntactic foam insulation coating.

The comparison between model simulations and experimental results is presented and discussed, that contributes to develop and complete a multiscale approach about multilayered coatings thermal performances characterisation. In complement, the sensitivities of the estimated thermal conductivity and the heat capacity values of the syntactic foam to several input parameters in the modelling have been studied.

One of the main objectives is to develop a useful model to predict the thermomechanical behaviour of complex multilayered structures submitted to ultra-deep service conditions, and thus determine if the coating system is well adapted to a particular field.

2. Experiments

2.1 Insulated pipe structure

The industrial structure (1.2m initial length) consists of a steel pipe (internal diameter of about 180mm, thickness about 18mm) and a 5-layers insulating coating (total thickness 61mm) which were industrially applied by side extrusion process, detailed by Berti (2004). The coating is composed of several material types: solid, adhesive polymers and syntactic foam, which is composed of hollow glass microspheres embedded in a polypropylene matrix. One advantage to combine varied materials is the possibility to obtain mechanical and thermal properties as well as good long term behaviour in water required for deep sea application, all these properties being difficult to obtain with a single material. The multilayered system and the materials thicknesses are presented in Figure 1.

Material	thickness (mm)
Steel pipe	18.26
Epoxy powder primer	0.25
Adhesive PP	0.25
Solid PP	3
Syntactic PP	55
Solid PP	2.5



The image shows a cross-section of a pipe with a central hole. The innermost part is a dark grey steel pipe. Surrounding it is a thick, multi-layered white insulation coating. Two arrows point from the text labels 'Steel pipe' and 'Insulation coating' to their respective parts in the image.

2.2 Material properties

Thermal and mechanical properties of each constitutive material of the test section are reported, respectively, in Table 1 and Table 2.

Material	Thermal conductivity ^{a)} (W.m ⁻¹ .K ⁻¹)	Heat capacity ^{a)} (J.kg ⁻¹ .K ⁻¹)
Steel pipe	45	475
Fusion bonded Epoxy	0.3	2000
Adhesive PP	0.22	2090
PP	0.22	2000
Syntactic PP	$0.165 + 10^{-4} \times T$ ^{b)}	$1506.6 + 6.26 \times T$ ^{b)}
Steel (cap) – APX4	19	460
PTFE (insulating end cap)	0.24	1050

a) Values are given at 20°C when the temperature dependence is not specified

b) The temperature is in °C

Table 1-Thermal properties

Material	Density (kg.m ⁻³)	Elastic modulus ^{a)} (GPa)	Poisson coefficient	Expansion coefficient (between 10 and 100 °C) (°C ⁻¹)
Steel pipe	7850	218	0.33	1×10^{-5}
Fusion bonded Epoxy	1200	3	0.4	5.3×10^{-5}
Adhesive PP	900	1.3	0.4	1.6×10^{-4}
PP	900	1.3	0.4	1.6×10^{-4}
Syntactic PP	640	$E = -0.94 \times 10^{-3} T + 1.1$ ^{b)}	0.32	5×10^{-5}
Steel (cap) - APX4	7700	211	0.33	1×10^{-5}
PTFE (insulating end cap)	2200	0.4	0.46	1.3×10^{-4}

a) Values are given at 20°C when the temperature dependence is not specified

b) The temperature is in °C

Table 2-Mechanical and thermomechanical properties

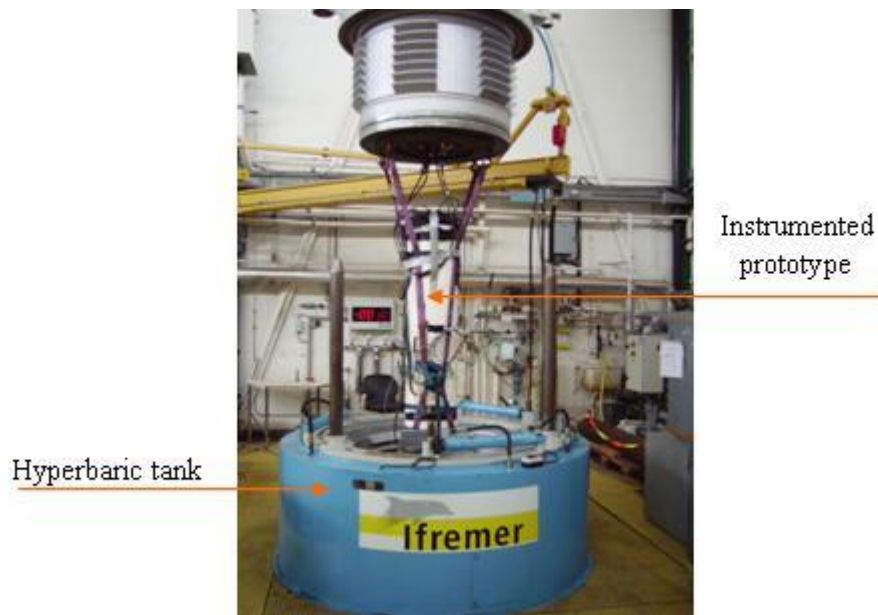
The values given for the PP syntactic foam were collected from experimental measurements performed at 1bar on small samples by Lefèbvre et al. (2006). For the steel pipe and the polymers, values from the literature were used as input data in the simulation.

2.3 In service tests

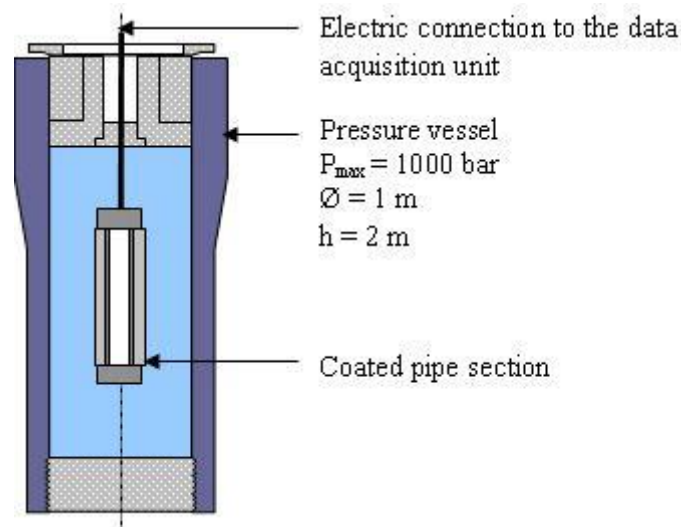
Experimental tests on the industrial prototype contribute to develop and complete a multiscale approach by collecting experimental data on an entire structure tested under representative service conditions of pressure and temperature. The tests also contribute to discuss the validity of the numerical modelling.

2.3.1 Testing facilities

For the prototype testing, a high pressure vessel (1m diameter, 2m height, up to 1000bar) located in IFREMER Brest was used (Figure 2).



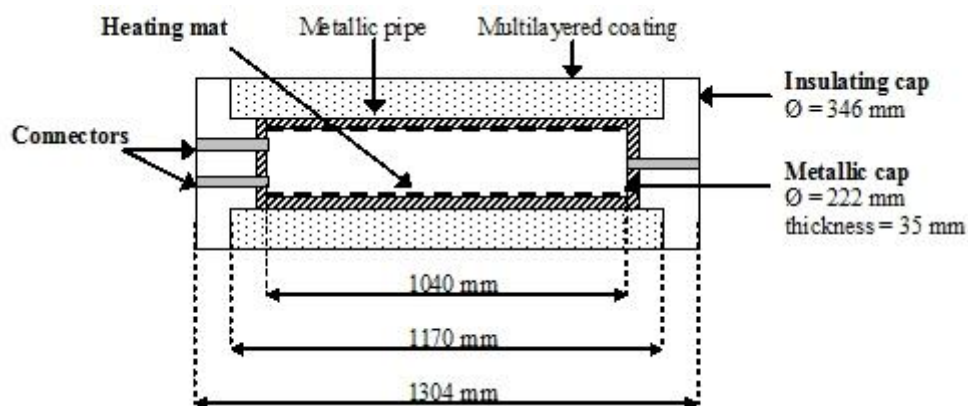
The pressure inside the vessel is regulated and monitored using a pressure transducer mounted at the top of the pressure vessel. The water temperature inside the pressure tank (about 15°C in this study) is also regulated and monitored during the tests. A schematic view of the coated test pipe in vertical position during testing in the pressure vessel is given in the Figure 3. The number of sensors for the prototype instrumentation was limited by the number of connections available on the pressure vessel flange.



2.3.2 Equipment

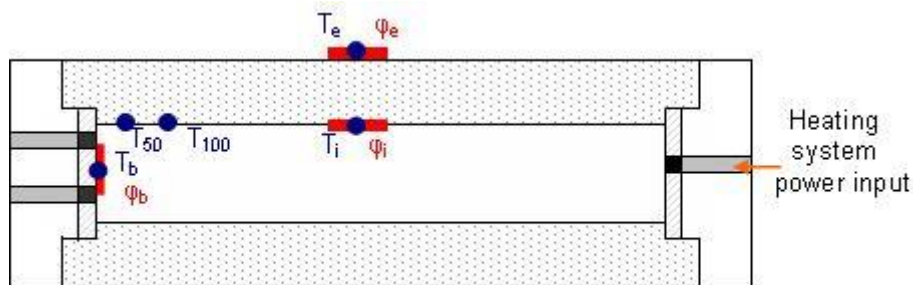
The insulated pipe section was machined at both ends to adapt two metallic steel caps in Stainless steel (APX4) covered by 100mm thick Polytetrafluoroethylene (PTFE) insulating caps in order to limit axial heat flow losses. The metallic caps were also equipped with connectors resistant to high external pressure. Three 10-channels connectors were necessary to allow the electrical supply of the inner heating system (one connector) and to collect inner sensor data (two connectors).

In this study, an original heating system was developed instead of the classical circulating oil to limit the convection effects inside of the pipe. The heating system consisting of heating elements (Nickel-Chrome wires) embedded in a thin silicone layer was placed on the internal diameter of the steel pipe and kept in place in contact with internal surface of the pipe by an inflatable silicon system. It is worth noting that such an inner 'dry' configuration with no pressure and no liquid is also very beneficial for the instrumentation used inside the pipe and will simplify the modelling of the inner heat flux boundary condition. In addition, this solution allows an easier control of the heating flow through the coating. The different elements that equipped the prototype are shown on Figure 4.



2.3.3 Instrumentation

The schematic representation of the fully instrumented pipe section and the location of sensors are given in Figure 5.



The insulated pipe section was instrumented with six commercial temperature sensors (Pt100) specified up to 200°C minimum (accuracy of about 0.3 % at 100 °C), located in both inner and outer parts along the pipe length and on the caps (Figure 5):

- T_i (°C): inner temperature of the steel surface in the center of the pipe (one measurement);
- T_e (°C): outer temperature of the coating surface in the center of the pipe (one measurement);
- T_b (°C): inner temperature of the steel surface in the center of one cap (one measurement);
- T_{100} (°C): inner temperature of the steel surface along the pipe 100mm distant from cap (one measurement);
- T_{50} (°C): inner temperature of the steel surface along the pipe 50mm distant from cap (one measurement);

Besides, the outer temperature of the water in the vessel, T_{water} (°C), was also measured using a platinum sensor.

The insulated pipe section was also instrumented with four commercial heat flux sensors located in both inner and outer parts along the pipe length and the caps:

- ϕ_i ($\text{W}\cdot\text{m}^{-2}$): inner thermal flux density on the steel surface in the center of the pipe (one measurement with soft circular fluxmeter of $5\mu\text{V}\cdot\text{m}^2\cdot\text{W}^{-1}$ sensitivity specified up to 200°C);
- ϕ_e ($\text{W}\cdot\text{m}^{-2}$): outer thermal flux density on the coating surface in the center of the pipe (three measurements with a semi-rigid fluxmeter of $50\mu\text{V}\cdot\text{m}^2\cdot\text{W}^{-1}$ sensitivity specified up to 100°C and 100bar (one measurement with a rigid fluxmeter of $30\mu\text{V}\cdot\text{m}^2\cdot\text{W}^{-1}$ sensitivity specified up to 250°C and 150bar);

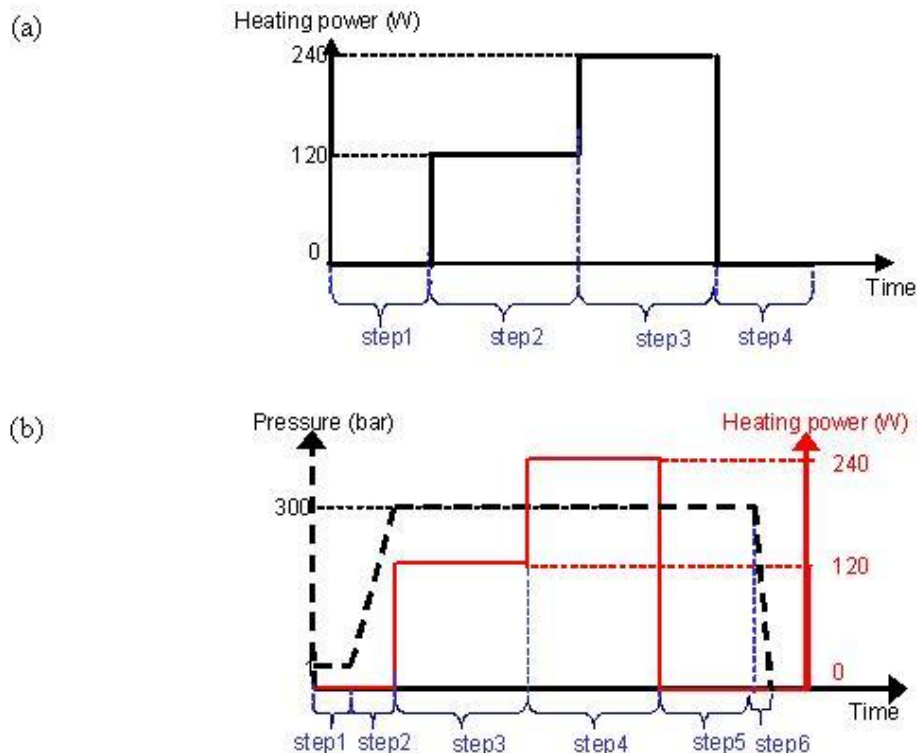
- ϕ_b ($\text{W}\cdot\text{m}^{-2}$): inner thermal flux density on the steel surface in the center of the steel cap (one measurement with rigid rectangular fluxmeter of $36\mu\text{V}\cdot\text{m}^2\cdot\text{W}^{-1}$ sensitivity specified up to 200°C).

Heat flux sensors with soft flat form were selected for the internal and external pipe surfaces to reduce errors related to the difficulties in mounting rigid flat sensors.

The readings obtained from all the sensors were recorded by a data acquisition unit which could be programmed to take recordings at appropriate time intervals throughout the duration of the test.

2.3.4 Testing procedures

For the experimental testing, a prototype structure has been instrumented and tested successively without additional pressure (external pressure of 1bar - test A) and under 300bar hydrostatic pressure (test B), simulating in-service conditions at about 3000m depth, at two different conditions of inner temperature, in order to study the influence of pressure and temperature on the thermal performances of the structure. Both test sequences programs are shown in Figure 6.



The details of each step are given in Table 3. The tests sequences have been chosen in order to be representative of service conditions (pressure then temperature). In both cases, it should be emphasized that a test lasting approximately 10 days cannot be used to predict the long term

evolution of the insulation coating systems for which water uptake and creep cannot be neglected.

Test	Step	Approximate duration	Pressure (bar)	Heating power (W)	Description
A	1	1 day	1	0	Stabilization at T_{water}
	2	3 days	1	120	Establishment of the stationary state 1bar/120W
	3	3 days	1	240	Establishment of the stationary state 1bar/240W
	4	2 days	1	0	Cooling and stabilization at T_{water}
B	1	1 day	1	0	Stabilization at T_{water}
	2	30 min	1 to 300	0	Pressure increase (until 300bar)
	3	3 days	300	120	Establishment of the stationary state 300bar/120W
	4	3 days	300	240	Establishment of the stationary state 300bar/240W
	5	3 days	300	0	Cooling at 300bar
	6	30 min	1 to 300	0	Pressure decrease

Table 3-Details of the test sequences

3. Theory of heat transfer

In parallel to experimental testing, a finite element modelling of the insulated pipeline has been developed in order to satisfactorily predict the thermomechanical behaviour of the structure when submitted to hydrostatic pressure and internal heating. Then an optimisation program based on analytical considerations has been developed to assess both thermal conductivity and heat capacity of the syntactic foam for several test conditions of temperature and pressure. These two complementary modelling approaches notably permit to evaluate the thermal parameters of the material studied (syntactic foam) even in the absence of any external heat flux sensor, in particular under 300bar hydrostatic pressure since commercial sensors are limited to a lower pressure range.

3.1 Transient state

The following analytical model describes the transient heat transfer by conduction in the prototype structure. In the case of a one-dimensional radial transfer in a one-layer structure limited by radii $r=r_{\text{int}}$ and $r=r_{\text{ext}}$, the heat equations for temperature and heat flux are:

$$\frac{1}{r} \frac{\partial}{\partial r} \left(r \frac{\partial T}{\partial r} \right) = \frac{1}{a} \frac{\partial T}{\partial t} \quad \text{for } r_{\text{int}} < r < r_{\text{ext}} \quad (1)$$

and

$$\Phi = -\lambda S \frac{\partial T}{\partial r} \quad (2)$$

with $T=T_0$ for $t=0$,

Applying a Laplace transform to the variable t , these equations lead to:

$$\frac{d^2\theta}{dr^2} + \frac{1}{r} \frac{d\theta}{dr} - \frac{p}{a} \theta \quad (3)$$

and

$$\phi = -\lambda S \frac{\partial \theta}{\partial r} \quad (4)$$

The quadrupoles notation, given by Maillet et al. (2000), is well suited to relate the Laplace transforms of the temperatures and fluxes at inner and external boundaries obtained by solving the above equations:

$$\begin{bmatrix} \theta_{int} \\ \phi_{int} \end{bmatrix} = \begin{bmatrix} A & B \\ C & D \end{bmatrix} \begin{bmatrix} \theta_{ext} \\ \phi_{ext} \end{bmatrix} \quad (5)$$

θ_{int} et θ_{ext} correspond to the transforms of the inner and outer surface temperatures of the cylindrical structure respectively, and A , B , C and D are analytical relations involving Bessel functions and the geometrical characteristics of the structure described by Maillet et al. (2000).

By applying this development to a multilayered pipeline structure submitted to outer convective losses, the equation (5) becomes:

$$\begin{bmatrix} \theta_{int} \\ \phi_{int} \end{bmatrix} = \prod_{i=1}^6 \begin{bmatrix} A_i & B_i \\ C_i & D_i \end{bmatrix} \begin{bmatrix} 1 & \frac{1}{h_{ext} S_{ext}} \\ 0 & 1 \end{bmatrix} \begin{bmatrix} \theta_{water} \\ \phi_{convective} \end{bmatrix} \quad (6)$$

with θ_{water} and $\phi_{convective}$ the Laplace transforms of the water temperature and the convective heat flux respectively.

With the boundary condition at the prototype-water interface:

$$-\lambda_6 \frac{\partial T}{\partial r} = h_{ext} (T_{water} - T(r = r_{ext}, t)) \quad (7)$$

The internal temperature variations $T_{int}(t)$ are calculated in the time domain by numerical inversion of the Laplace transform θ_{int} , given by Stehfest (1970).

3.2 Steady state

For a one-dimensional conduction problem in a cylindrical structure, the analytical expression for the radial heat flux in steady state conditions is linked to the inner and outer surface temperatures and to the global heat transfer coefficient U of the structure (evaluated on the inner surface of the structure taken as reference) by the following relation:

$$Q = -U.S. (T_{ext} - T_{int}) \quad (8)$$

For a multilayer structure, and by assuming that the thermal contact resistance between each layer can be neglected, the global heat transfer coefficient U of the structure can be expressed in terms of constitutive material thermal conductivities with the following relation:

$$U = \frac{1}{S \times \sum_{i=1}^n \left[\frac{\ln\left(\frac{D_{i+1}}{D_i}\right)}{2\pi L \lambda_i} \right]} \quad (9)$$

This coefficient is a representative thermal characteristic of the entire system: steel pipe and insulation coating, which represents the thermal performance of the multilayered structure.

4. Numerical modelling

4.1 Model assumptions

The thermomechanical modelling of the prototype structure was performed with the software Comsol Multiphysics[®], based on the finite element method, which is a tool particularly well adapted for coupling problems between several phenomena. The modelled structure is based on the real geometry of the multilayered insulated pipe. The thermal contact resistance between each layer is assumed to be negligible. The structure is assumed to be without structural defects, so the modelling was performed in 2D-axisymmetric geometry. The electric connectors placed in the end caps are here not considered to ensure symmetry conditions (same end caps). This allows to model only the half of the prototype structure and thus to increase the number of elements. The finite element model is based on three node elements. The experimental prototype tests were performed during a relatively short duration, therefore, the water diffusion and also creep aspects are here neglected. These hypotheses also simplify considerably the modelling, decrease the time of calculation, and allow refining the mesh and also increasing the element number for the solution. At this stage of the study, the syntactic foam has been considered as a linear elastic material, with thermal and mechanical properties depending on the temperature. More complete models are under development.

The temperature distribution in the steel pipe and on the insulation coating system was determined during all test sequences. Moreover, thermal heat flux on the external surface of the structure or deformation of each material layer could also be determined.

In order to evaluate the influence of the internal thermal boundaries on the simulation of the thermomechanical behaviour of the structure, two models of the entire structure were

developed. The first takes into account the phenomenon of thermal conduction in the air localised inside of the pipe, and the second considers the phenomenon of thermal convection between the metallic surfaces and the internal air.

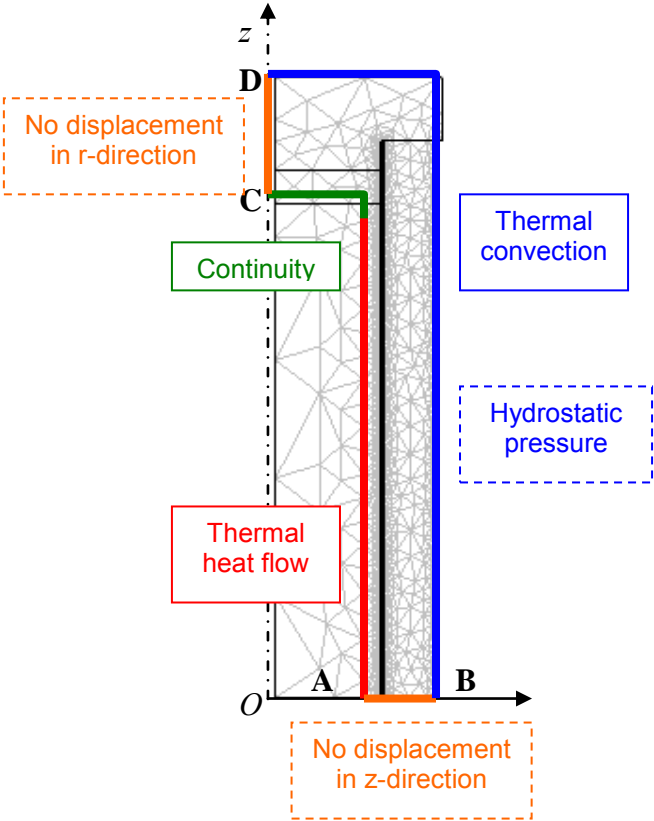
For both Comsol models (internal conduction or convection), the initial conditions of temperature and pressure depend on each test sequence performed on the structure. The finite element model is based on three node elements and the mesh was locally refined near interfaces and sensors to enhance the resolution.

4.2 Boundary and initial conditions

4.2.1. Comsol models

a) Internal conduction

The geometry of the computational domain, the numerical mesh and the boundary conditions of the two models are shown in Figure 7. In this model, the air is considered as a stagnant and purely conductive media. The thermal properties of the air considered in the model are from Holman (1983).



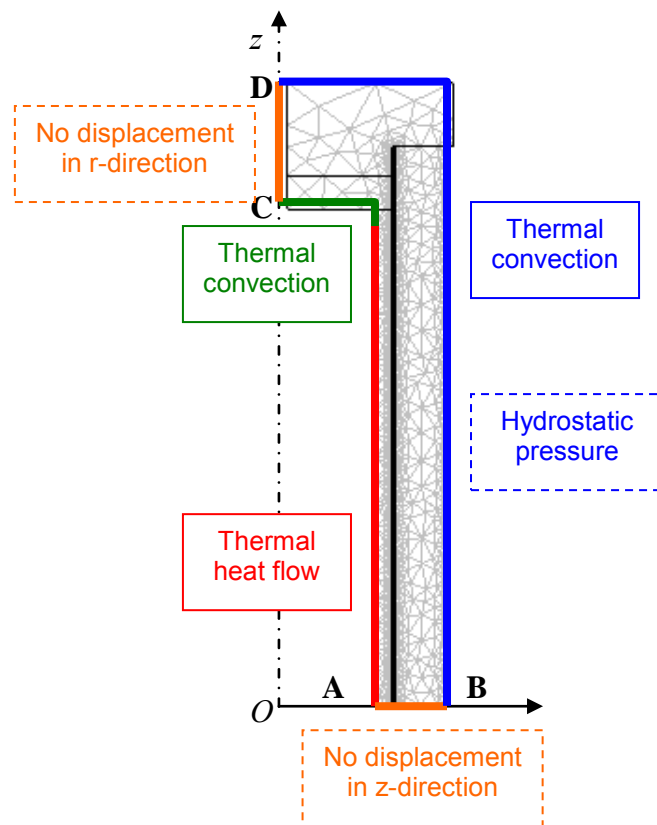
The boundary conditions are:

- no displacement in z-direction for the lower section (A-B) and no displacement in r-direction for the upper section (C-D);

- thermal heat flow density condition on the inner surface of the steel pipe (heating map);
- for the external convection condition, the convection coefficients were calculated from experimental temperatures T_e and T_{water} , as described by Eyglunent (1997);
- continuity (of temperature and flow) at the interface between the internal air and the internal surfaces (heating map and metallic surfaces).
- For tests under hydrostatic pressure, an additional stress condition is applied on the external surfaces of the structure.

a) Internal convection

The geometry of the computational domain, the numerical mesh and the boundary conditions of the two models are shown in Figure 8. This second model is based on the hypothesis of thermal convection between the air and the interne metallic surfaces.



The boundary conditions are:

- no displacement in z-direction for the lower section (A-B) and no displacement in r-direction for the upper section (C-D);
- thermal heat flow density condition on the inner surface of the steel pipe (heating map);

- for the external convection condition, the convection coefficients were calculated from experimental temperatures T_e and T_{water} , as described by Eyclunent (1997).
- natural convection along the internal surfaces at both inner end metallic caps in contact with air and natural convection along the external surfaces in contact with water. For the internal convection condition, the convection coefficients were calculated from experimental temperatures - temperature in the centre of the metallic cap (T_b) and initial temperature of the structure ($T_{inicial}$), as described by Evans and Stephany (1965) or Holman (1983), who described the calcul of the Nusselt coefficient in the case of natural convection phenomenon in closed vertical or horizontal cylinders. The Nusselt coefficient is calculated with the following relation:

$$Nu=0.55 \times (Gr \times Pr)^{1/4} \quad (10)$$

With:

Gr: the Grashof number

Pr: the Prandtl number

And the convection coefficient h is determined by:

$$h=Nu \times \lambda / L \quad (11)$$

With:

λ : the thermal conductivity of the internal air

L: the length of the cylinder

- For tests under hydrostatic pressure, an additional stress condition is applied on the external surfaces of the structure.

c) Matlab routine

Both thermal conductivity and heat capacity can be determined by an optimisation program developed with software Matlab[®] with an indirect method relying on an inverse methodology. This routine allowed the evolution of the inner temperature of the steel pipe T_i to be adjusted during the testing time simulated by an analytical relation to the experimental data by optimisation (square root method) of the thermal parameters of the material studied, here the syntactic foam. Temperatures and heat fluxes evolutions are obtained in the time space by means of the numerical inversion of each Laplace transform. Transient model hypotheses are:

- One-dimensional axisymmetric;
- Constant convective heat transfer coefficient and water temperature;
- Constant internal heat flux equal to the value of the steady state heat flux in the structure;

- Initial temperature of the entire structure supposed to be stabilized at the water temperature;
- The inner and outer radius of each layer are taken from the numerical modelling results obtained in stationary state with Comsol Multiphysics[®] (in order to take into account thermal expansion and pressure effect on each material thickness).

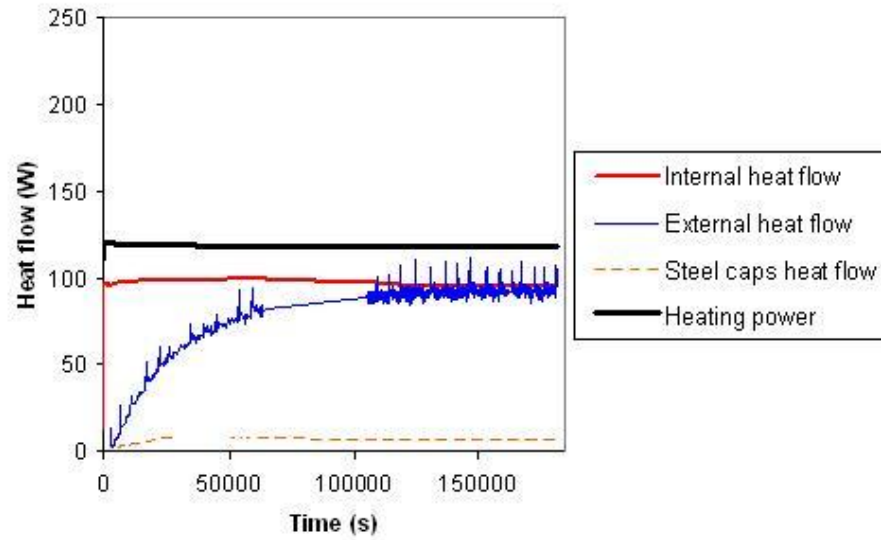
5. Results and discussion

5.1 Validation of the numerical modelling

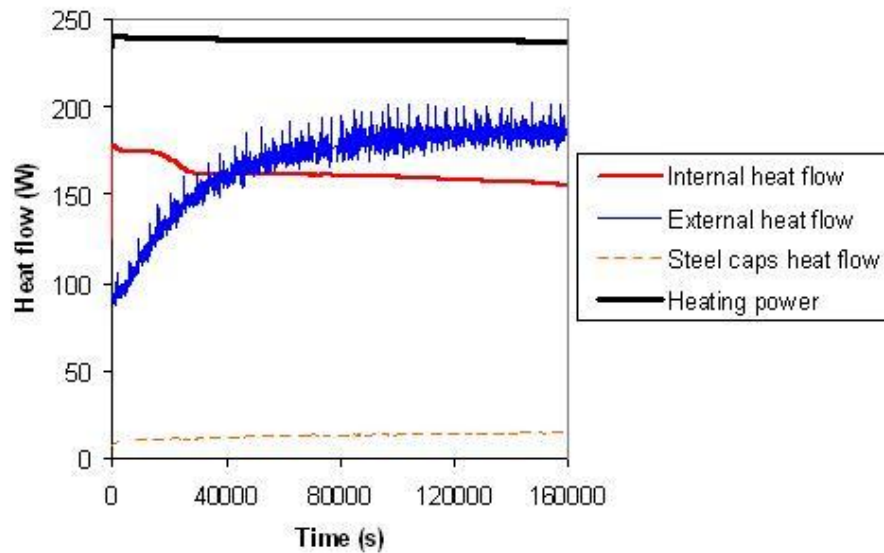
5.1.1 Instrumentation limits

During the prototypes testing, some experimental measurement problems of the fluxmeters could be highlighted. The fluxmeters seem to lose sensitivity when the temperature increases. Figure 9a shows that at 120 W heating power (corresponding to a relative low inner temperature: about 50 °C), the inner fluxmeter measurements are comparative to the heating power registered. But when the heating power increases (inner temperature of about 95 °C), the difference between the heating power value and the inner flow measurement increases as well (Figure 9b). The internal heat flow values are at least approximately 16% smaller than the heat flow that exits from the pipe, which underlines the difficulty to obtain experimentally a precise internal heat flow. The fluxmeter localised at the center of the metallic cap also registered relative low values. This fluxmeter was placed at the interface between the metallic cap and the internal air that could explain the difficulty to obtain pure conductive heat flow. It shows the limitation of using a single fluxmeter in this position in order to evaluate the heat losses at the end caps. Therefore simulations results will be very used in this work to evaluate external heat flows, and also axial heat losses.

(a)



(b)

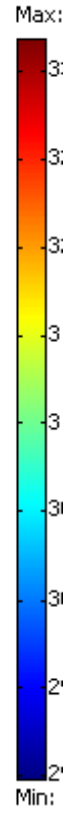
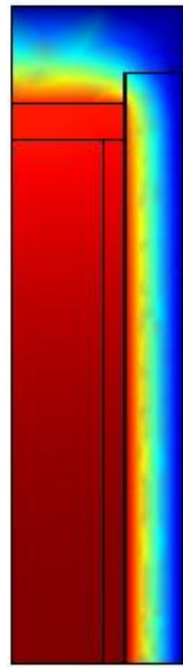


5.1.2 Modelling results

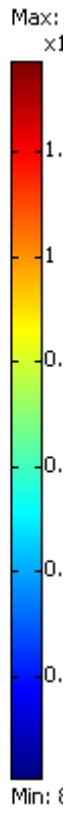
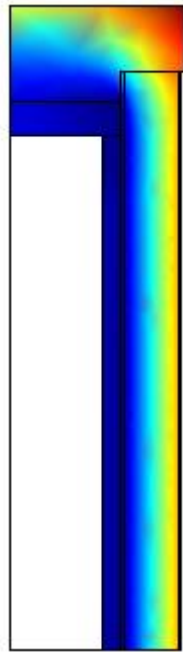
Internal heat flux densities were calculated from the aforementioned heat fluxes (respectively 120W or 240W) by dividing flux values by 0.57m^2 (internal heating mat surface area). Both simulations of thermomechanical behaviour of the insulated pipe section were performed with those calculated internal flux densities.

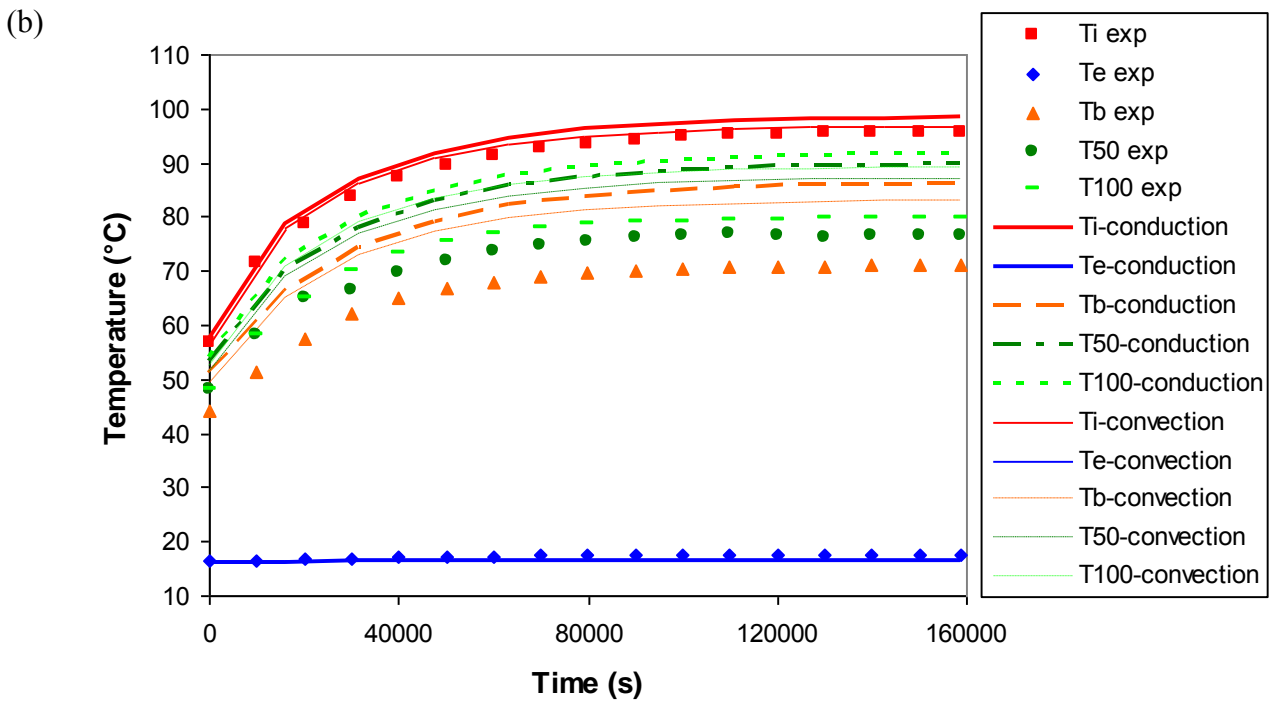
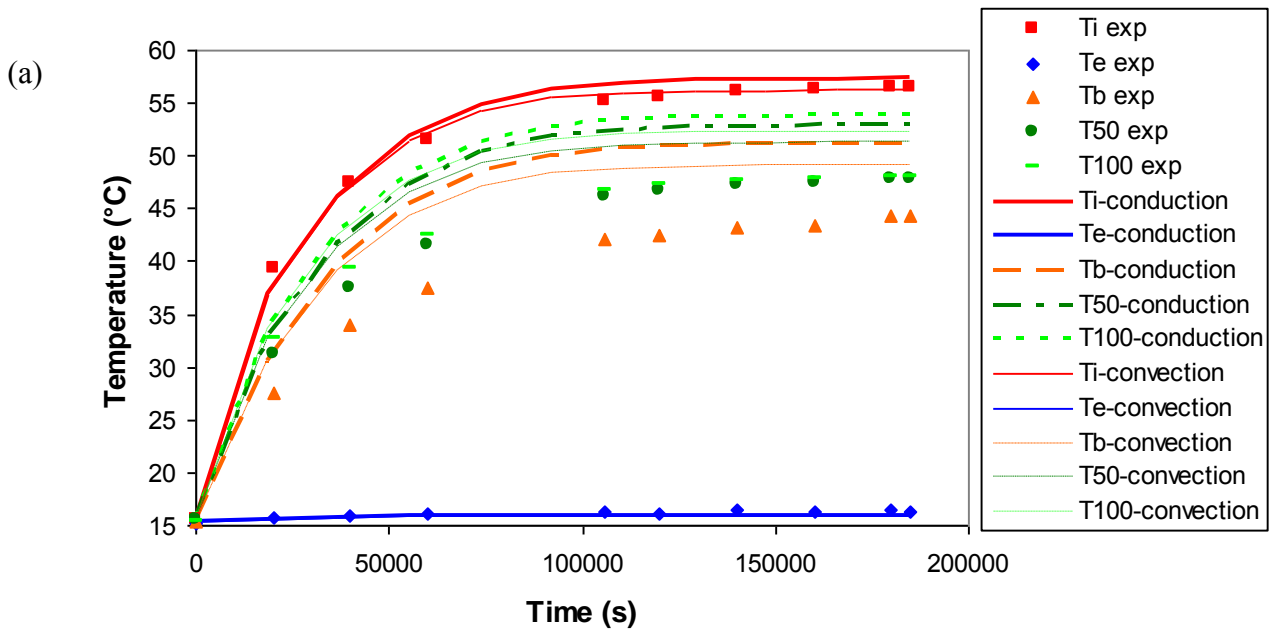
The temperature and the displacement distributions simulated within insulated pipe section with the model based on internal conduction is shown in Figure 10a (temperature) and Figure 10b (total displacement), for the case 300bar, 120W.

(a)



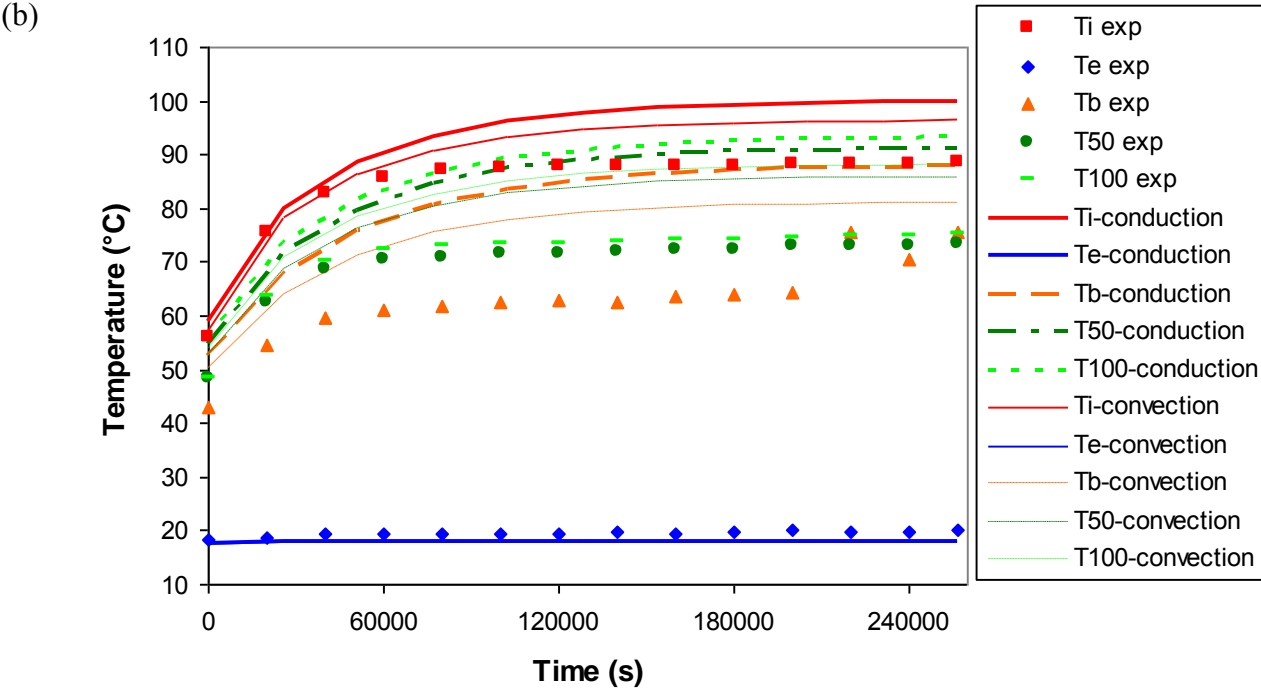
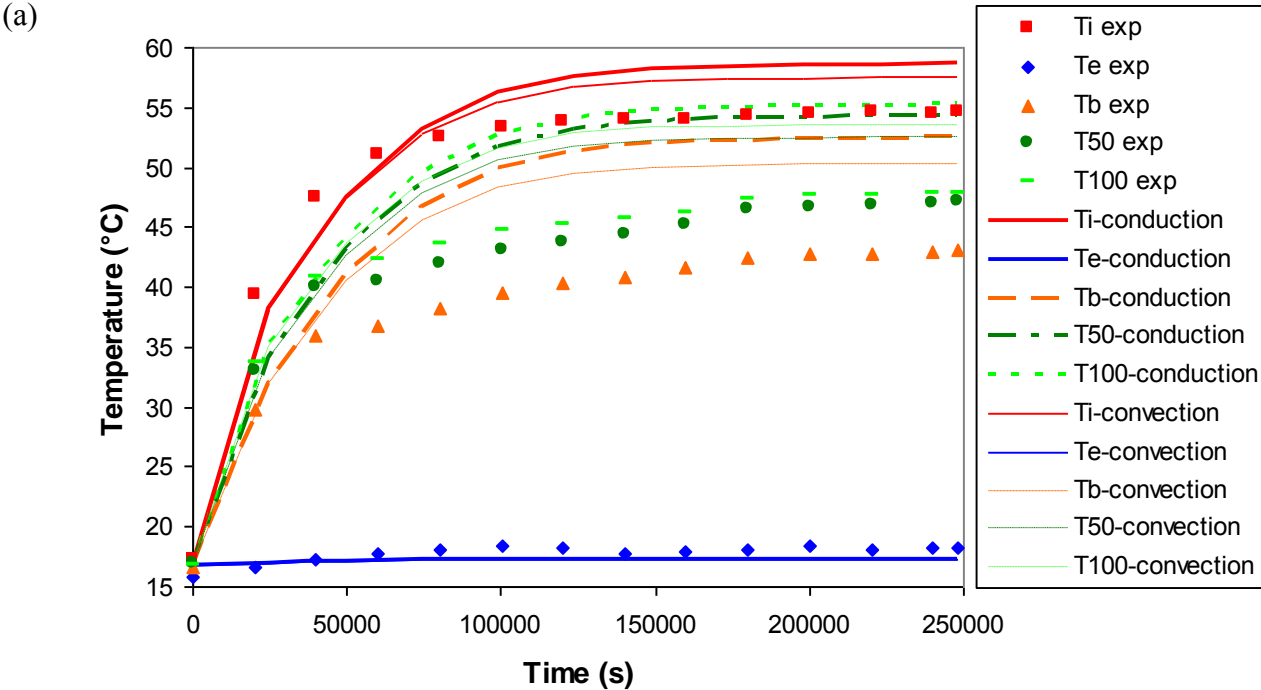
(b)





One can notice that for both tests (heating power of 120W and 240W), the simulated interne and externe temperatures T_i and T_e fit quite well the experimental values, in particular for the convection model. The other simulated temperatures (T_b , T_{50} and T_{100}) are significantly overestimated (more than 10 °C difference for T_b in step 3 – Figure 10b). The results show that for each condition, the convection model fits better the experiments than the conduction model.

The same remarks could be highlighted for the tests realized under 300bar, illustrated in the Figure 13, where the differences between experimental and simulated temperatures are even higher. The difference observed between experimental and simulated values could be in part explained by the difficulty to determine the thermal convection coefficients (external and internal surfaces).



5.2 Estimation of insulation thermal properties

5.2.1 Steady state modelling

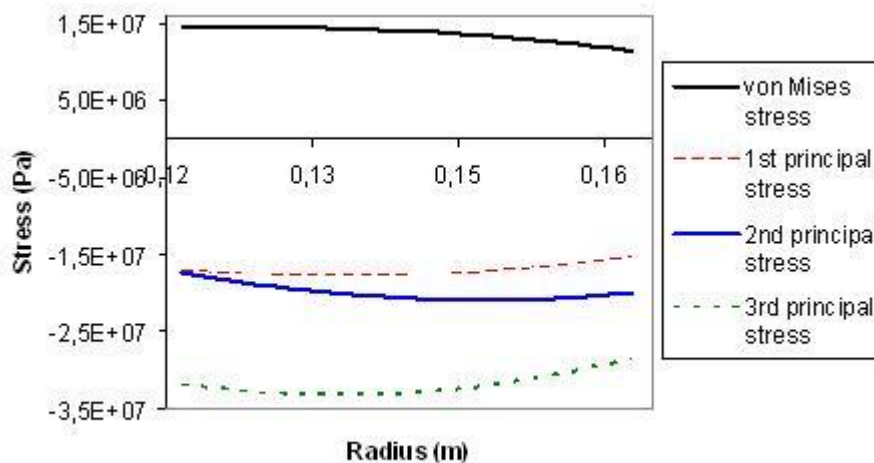
In the absence of any external heat flux sensor, the external heat flux could be approached by simulation. For each test sequences, the heat transfer coefficient U has been determined using equation (8) directly from measured temperatures and simulated external radial heat fluxes, for both Comsol models (internal conduction or convection). The external heat flux is determined by integrating the heat flux densities on the external surface of the pipe, considering the length of the pipe that is directly submitted to the heating (1m length as for the heating mat dimension). Then the apparent thermal conductivity of the syntactic PP (corresponding to the thermal conductivity of the syntactic PP averaged on the insulation cross section under thermal gradient) is derived from equation (9). Calculated U values and apparent thermal conductivities of syntactic PP are reported in the Table 4.

Test sequence	Pressure (bar)	Heating mat power (W)	Internal heat flux model ($W.m^{-2}$)	External radial heat flow (W)	Total external axial heat flow (W)	Total axial heat losses (%)	Ti ($^{\circ}C$)	Te ($^{\circ}C$)	U ($W.m^{-2}.K^{-1}$)	Apparent thermal conductivity of syntactic PP ($W.m^{-1}.K^{-1}$)
TestA step2 conduction	1	120	210	<i>97.3</i>	<i>22.9</i>	<i>19</i>	56.4	16.4	4.24	0,167
TestA step2 convection				<i>94.1</i>	<i>21.6</i>	<i>18</i>				
TestA step3 conduction	1	240	420	<i>194.7</i>	<i>45.5</i>	<i>19</i>	95.8	17.6	4.34	0,171
TestA step3 convection				<i>189.7</i>	<i>43.5</i>	<i>18</i>				
TestB step3 conduction	300	120	210	<i>97.3</i>	<i>22.8</i>	<i>19</i>	55,6	18.3	4.68	0,186
TestB step3 convection				<i>93.9</i>	<i>21.5</i>	<i>18</i>				
TestB step4 conduction	300	240	420	<i>194.8</i>	<i>45,3</i>	<i>19</i>	88.5	20	4.96	0,198
TestB step convection				<i>184.22</i>	<i>41.4</i>	<i>17</i>				

Table 4-Heat flows and temperatures in the steady state and related thermal properties (simulation results are in italics)

The global heat transfer coefficient U estimated with both numerical models at 1 bar (internal conduction and internal convection) is comparative to the value given by the insulated pipe manufacturer (about $4.2 \text{ W} \cdot \text{m}^{-2} \cdot \text{K}^{-1}$ at 20°C and 1 bar, according to the thermal characteristics given by the manufacturer), which validates the use of the thermomechanical numerical simulation to determine the global heat transfer coefficient U and the apparent thermal conductivity of insulation materials. The results also highlight that the apparent thermal conductivities of syntactic PP are slightly lower than values measured on small specimens (given in Table 1).

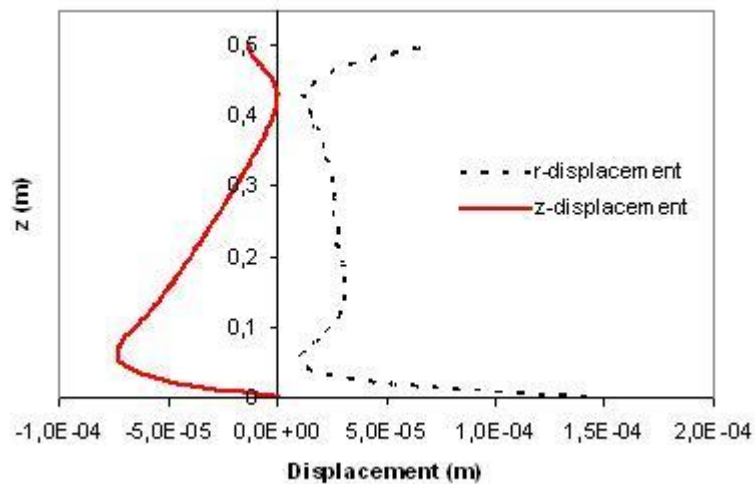
For the test sequences realized at 1bar pressure, simulated results show that U values and apparent thermal conductivities do not seem to be significantly influenced by the high inner steel temperature. For the test sequences realized at 300bar pressure, simulated results show that U values and apparent thermal conductivities increase in relation to the tests realized at 1 bar, and the values also seem to be slightly influenced by the high inner steel temperature. The relative increase of the U value (about 10% increase between tests at 1 bar and tests at 300bar) and related increase of the apparent thermal conductivity could be explained by damage occurring in the foam microstructure, in particular near the steel pipe where material is subjected to coupled effect of high temperature and complex stress distribution. The Figure 14 represents the stress repartition along the syntactic foam thickness in the middle plan of the structure, obtained with Comsol Mutiphysics[®], when the prototype is submitted to high hydrostatic pressure (300bar) and high inner heating power (240W).



The results show that the von Mises stresses in the syntactic foam are not negligible, in particular near the metallic pipe, and that the values of the three principal stresses are very different, which underlines the anisotropy of the mechanical loads applied to the prototype structure. Therefore it exists deviatoric stresses in the thickness of the multilayer coating that

could induce damage, particularly in the structure of the syntactic foam. This damage could conduct to an evolution of the mechanical properties of the foam (Young's modulus E , coefficient de Poisson ν) during the tests and thus explain the relative increase of the thermal conductivity of the foam.

To complete this point, the respective displacements in the radial direction (r) and in the vertical direction (z) obtained with the Comsol Multiphysics[®] simulation at the interface between the solid PP layer and the internal surface of the syntactic foam (near the metallic pipe) in the steady state (300bar/240W) are represented along the half structure in Figure 15.

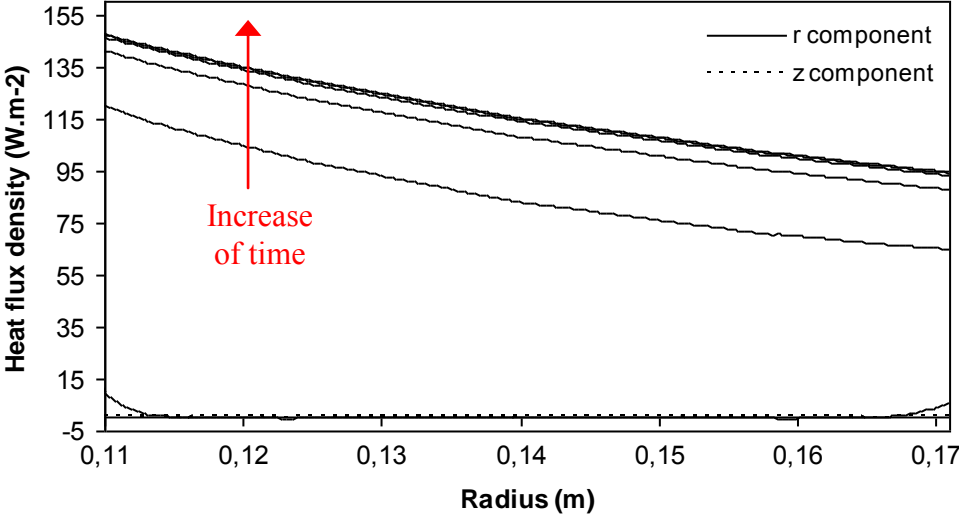


It illustrates the notable differences in the displacements values along the structure, resulting from the coupling of high internal heating and high external hydrostatic pressure. However, it is important to keep in mind that the thermal parameters (global heat transfer coefficient and apparent thermal conductivity of the syntactic foam) were based on simulation results (simulated external heat flow at the stationary state) and on experimental temperatures. Therefore it is very delicate to evaluate the level of uncertainty of the values obtained.

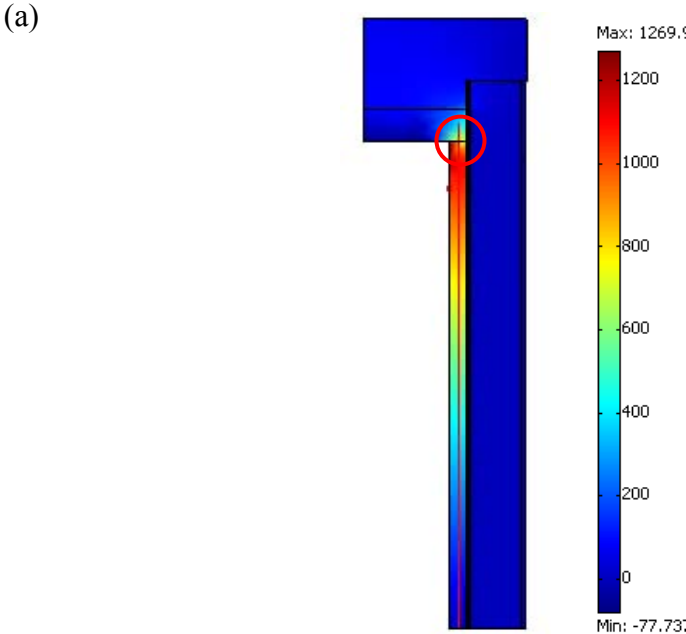
5.2.2 Transient case

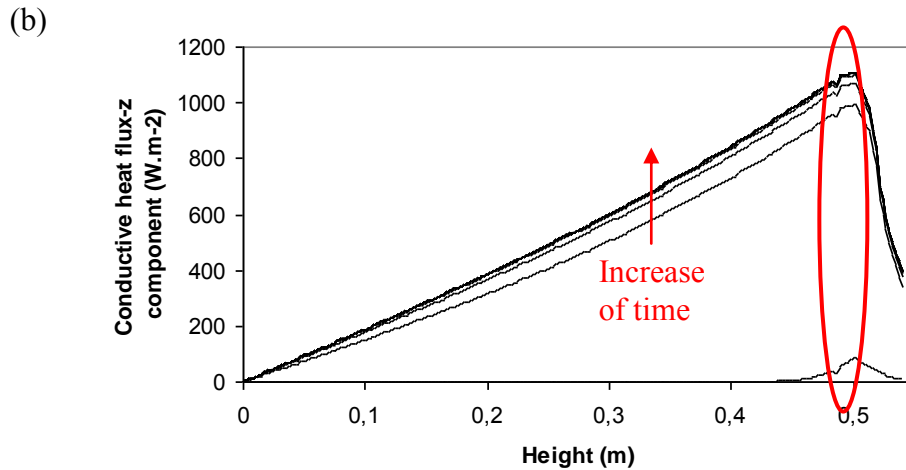
For the simulations based on the Matlab routine, the inner heat flux density feeding the model was determined with Comsol. The model with internal convection relatively better fit experimental temperatures than the conductin model. Therefore, we determined the heat flux density based o the results of internal convection. The hypothesis of 1D-axisymmetric used for the Matlab routine could be justified for a first approach by the repartition of the heat flux through the thickness of the coated pipe. The radial and axial component of the conductive heat flux in the center of the stucture is represented in Figure 16, at several times of the

modelling (hypothesis of internal convection). We can observe that in the center of the structure, the axial component of the heat flux through the metallic pipe and the coating is negligible in regards to the radial component.

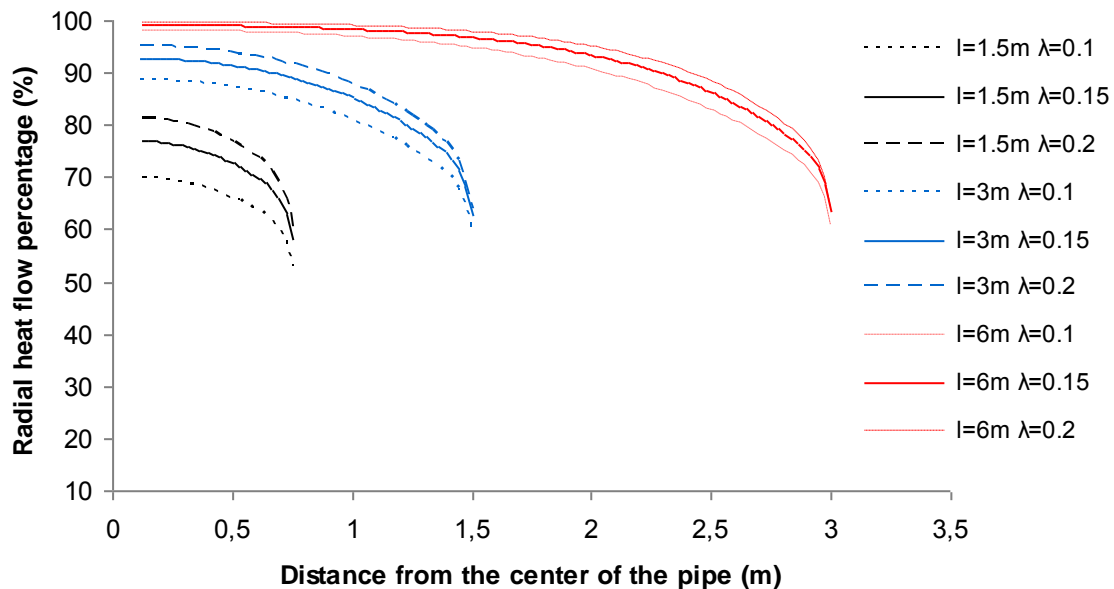


The axial component of the conductive heat flux in the structure obtained with Comsol is presented in Figure 17. The simulations results show that the axial component of the conductive heat flux increases along the pipe, and is maximum at the interface between the pipe and the metallic cap (circled area).



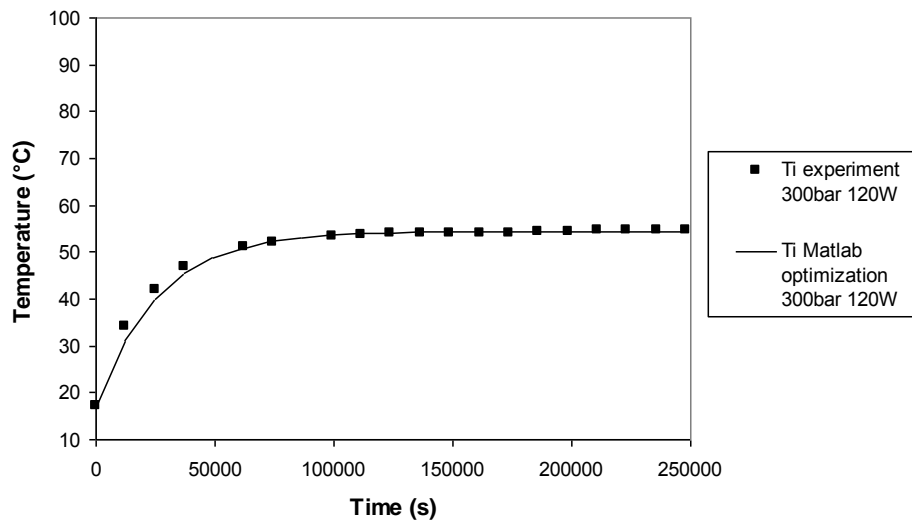


A parametric study about the heat flux repartition was also realized in order to illustrate the influence of pipe length and thermal conductivity of the material on the radial heat flow percentage (Figure 18). For different pipe length (1.5m, 3m and 6m), and different thermal conductivity of the insulation coating (0.1, 0.15 and 0.2 W.m⁻².K⁻¹), the percentage of radial heat flow was determined from numerical simulations. The results show that the nearest from the center of the structure, the higher are the radial heat flow percentage. In the case of a relative short pipe (1.5m length), the radial heat flow percentage in the center of the structure is between 70 and 80%, depending from the thermal conductivity considered.



Since the analysis of experimental data with the transient model approach requires that initial temperatures are fully stabilised, the evolution with time of the inner temperature could be simulated only for the two following testing sequences: test A/step 2 (1bar 120W) and test

B/step 3 (300bar 120W). The experimental values and simulated curves are compared on Figure 19. Optimisation input data and results are reported in the Table 5.



Test sequence	Pressure (bar)	Heating mat power (W)	Water temperature (°C)	Mean external convection coefficient ($\text{W}\cdot\text{m}^{-2}\cdot\text{K}^{-1}$)	Apparent thermal conductivity of syntactic PP ($\text{W}\cdot\text{m}^{-1}\cdot\text{K}^{-1}$)	Apparent heat capacity of syntactic PP ($\text{J}\cdot\text{kg}^{-1}\cdot\text{K}^{-1}$)
Test A step 2	1	120	15.3	125	0.150	1501
Test B step 3	300	120	16.7	170	0.154	1500

Table 5-Thermal properties of syntactic PP determined by the transient state analysis (simulation results are in italics)

The very similar apparent thermal conductivity values obtained compared to the steady state approaches validate the transient state analysis and its one-dimensional hypothesis.

One can notice that the apparent heat capacity of syntactic PP is lower than the value determined experimentally (heat capacity expression given in Table 1), and this later value should be considered with caution since temperature sensitivity to heat capacity variations is low.

From apparent thermal conductivity and heat capacity values obtained under 120W 1bar and 120W 300bar, there is no significant difference as stated previously from steady state analysis. Thus, one can conclude that the coupling effect between high hydrostatic pressure (300bar) and inner temperature of the metallic pipe at about 50 °C (corresponding to the inner

surface temperature measured in the steady state with 120W heating power input) induces negligible short term consequences on syntactic PP. But in the case of higher temperatures and above coupled with ultra deep service pressure, short term phenomena could occur in the syntactic PP leading to a lowering of insulation performance.

5.3 Sensitivity study

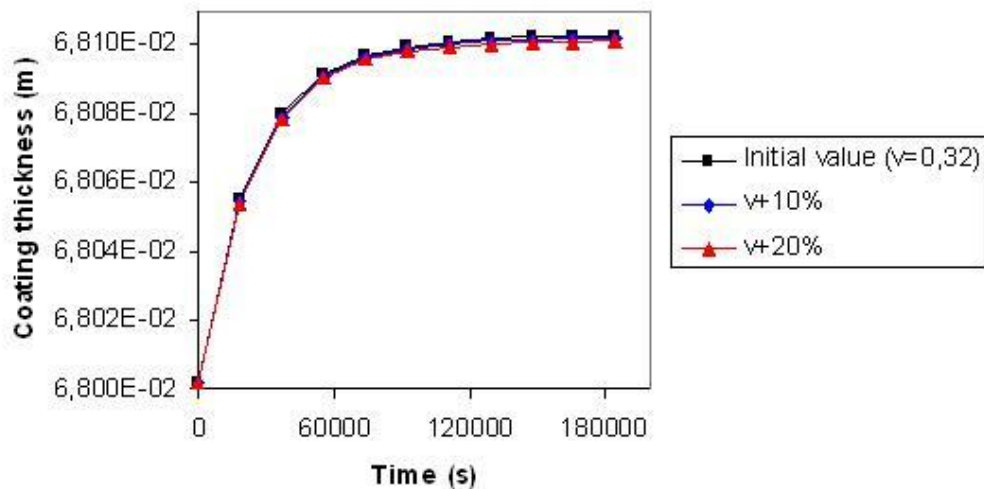
One parameter that appears interesting to considerate in the sensitivity study is the Poisson coefficient value of the syntactic foam, which is susceptible to change during the tests. In fact, the influence of temperature increase inside the syntactic foam during the different test sequences could probably induce an increase of the global Poisson coefficient value of the syntactic foam. This coefficient is directly linked to the deformation of the syntactic foam, and thus to the evolution of coating thickness. Therefore, the deformation of each material has been first calculated with the finite elements modelling (developed with Comsol Multiphysics[®]), then reported in the optimization routine to take into account the syntactic foam Poisson coefficient evolution. The optimization results are reported in Table 6, the corresponding coating thickness evolutions during each sequence are related in Figure 19.

Test sequence	Pressure (bar)	Heating mat power (W)	$v_{\text{syntactic PP}} +10\%$	$v_{\text{syntactic PP}} +20\%$
Test A step 2	1	120	$\lambda+0.15\%$ $C_p-0.05\%$	$\lambda-0.05\%$ $C_p-0.05\%$
Test B step 3	300	120	$\lambda+0.01\%$ $C_p\pm 0\%$	$\lambda+0.02\%$ $C_p\pm 0\%$

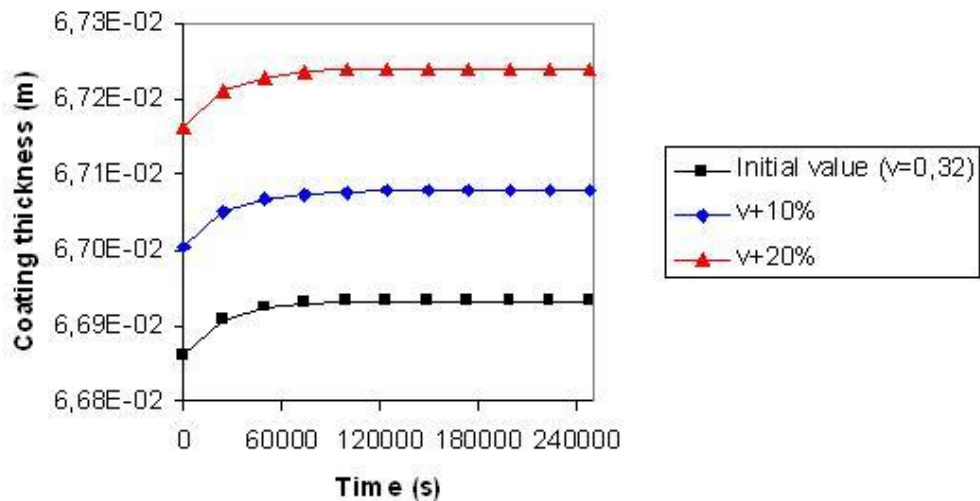
The notation “ $v\pm x\%$ ” signifies that the input thermal parameter v has been increased or decreased from $x\%$ in comparison to the initial input data in the optimisation routine.

Table 6-Influence of input Poisson coefficient of the syntactic PP on optimised thermal parameters of the syntactic foam

(a)



(b)



The optimised values obtained for the thermal properties of the syntactic foam reveal very low evolutions (up to 0.15% increase), that underlines the fact that with the hypothesis considered in the modelling, the Poisson coefficient variation do not affect significantly optimization results.

These graphics show that the syntactic foam Poisson coefficient evolution did not have a significant influence for the test realized at 1bar (influence of thermal expansion only), whereas at 300bar the coating thickness evolution is more marked due to the influence of thermal expansion and hydrostatic pressure (up to 0.5% increase).

In further studies, the evolution of the Poisson coefficient of the foam with temperature could also be included in the input parameters of the modelling directly as a function of the temperature, as it has been already done for the mechanical modulus.

6. Conclusions

Two thermomechanical models of a multilayered coated pipeline, alimeted with experimental data obtained on small syntactic foam samples, have been developed to predict the behaviour of the structure submitted to internal heating and external pressure. The first model considers internal thermal conduction and the second considers internal thermal convection between the metallic surfaces and the internal air. The validity of the models has been discussed through experimental results obtained during tests performed on industrial insulated pipes under service conditions (inner temperature up to 95°C and hydrostatic pressure up to 300bar). A method has been developed including FE analysis and analytical model to determine the thermal properties of the syntactic foam for several test conditions of temperature and pressure. Both models allow determining apparent thermal properties of the syntactic foam in accord with manufacturer data. The model based on internal convection fit better experimental data than the model based on internal conduction. To improve the modelling, complementary experimental tests should be realized in order to better evaluate the convection coefficients (internal and external convection conditions). A sensitivity study of the numerical modelling to the input Poisson coefficient of the syntactic foam has also been presented. This study demonstrates that the impact of this parameter evolution seems to be quite low on numerical results (less than 0.2% evolution in comparison with the initial values of syntactic foam thermal properties). Lastly, it should be mentioned that the next step to qualify multilayered insulated structures should be the development and realization of long term testing on an industrial pipe. To describe the long term behaviour of such prototypes, a hydro-thermo-mechanical model should also be developed and validate with experimental data, by taken into account the coupling between water diffusion, temperature and mechanical loads.

7. Acknowledgments

The authors wish to thank Socotherm for providing the insulated coated pipes, in particular G. P. Guidetti for his interest to this work and N. Lacotte and A. Deuff for the performing of hyperbaric tests.

8. References

- Berti, E., 2004. Syntactic polypropylene coating solution provides thermal insulation for Bonga risers, *Offshore Magazine*, **64**, 2.
<http://www.offshore-mag.com/currentissue/index.cfm?p=9&v=64&i=2>

- Bouchonneau, N., Sauvant-Moynot, V., Grosjean, F., Choqueuse, D., Poncet, E., and Perreux, D., 2007. Thermal Insulation Material for Subsea Pipelines: Benefits of Instrumented Full Scale Testing to Predict the Long Term Thermo-mechanical Behaviour. *Proceedings of the Offshore Technology Conference – OTC 18679*, Houston, Texas, USA.
- Choqueuse, D., Chomard, A., and Bucherie, C., 2002. Insulation materials for ultra deep sea flow assurance: Evaluation of the material properties. *Proceedings of the Offshore Technology Conference - OTC 14115*, Houston, Texas, USA.
- Choqueuse, D., Chomard, A., and Chauchot, P., 2004. How to provide relevant data for the prediction of long term behavior of insulation materials under hot/wet conditions? *Proceedings of the Offshore Technology Conference - OTC 16503*, Houston, Texas, USA.
- Choqueuse, D., Chauchot, P., Sauvant-Moynot, V., and Lefèbvre, X., 2005. Recent progress in analysis and testing of insulation and buoyancy materials. *Proceedings of the Fourth International Conference On Composite Materials for Offshore Operations - CMOO-4*, Houston, Texas USA.
- Evans, L. B. And Stephany, N. E., 1965. An experimental study of transient heat transfer to liquids in cylindrical enclosures. *Proceedings of the Heat Transfer Conference*, Los Angeles, USA.
- Eyglunent, B., 1997. *Manuel de thermique - Théorie et pratique*, HERMES Science Publications, Paris.
- Gimenez, N., Sauvant-Moynot, V., and Sautereau, H., 2005. Wet ageing of syntactic foams under high pressure / high temperature in deionized and artificial sea water. *Proceedings of the Twenty-Fourth International Conference on Offshore Mechanics and Artic Engineering*, Halkidiki, Greece.
- Haldane, D., Graff, F.v.d, and Lankhorst, A.M., 1999. A Direct measurement system to obtain the thermal conductivity of pipeline insulation coating systems under simulated service conditions. *Proceedings of the Offshore Technology Conference - OTC 11040*, Houston, Texas, USA, pp. 1-16.
- Haldane, D., Scrimshaw, K.H., 2001. Development of an alternative approach to the testing of thermal insulation materials for subsea applications. *Proceedings of the Fourteenth International Conference on Pipeline Protection*, Barcelona, Spain, pp 29-39.
- Holman, J., 1983. Heat Transfer. Mcgraw-Hill Series in Mechanical Engineering.
- Lefèbvre, K., Sauvant-Moynot, V., Choqueuse, D., and Chauchot, P., 2006. Durabilité des

matériaux syntactiques d'isolation thermique et de flottabilité: des mécanismes de dégradation à la modélisation des propriétés long terme. *Proceedings of the Conference: Matériaux 2006*, Dijon, France.

Maillet, D., André, S., Batsale, J.C., Degiovanni, A., and Moyne, C., 2000. *Thermal quadrupoles : solving the heat equation through integral transforms*, John Wiley & Sons, Inc.

Robertson, S., Macfarlan, G., and Smith, M., 2005. Deep water expenditures to reach \$20 billion/year by 2010, *Offshore Magazine*, **65**, 12.

<http://www.offshore-mag.com/currentissue/index.cfm?p=9&v=65&i=12>

Stehfest, H., 1970. Algorithm 368 : Numerical inversion of Laplace transform, *Communication of the ACM* **13**, 1.

9. Figure legends, figures, tables

Figure 1. Industrial 5-layers insulation system

Figure 2. Setting up of the instrumented prototype in the hyperbaric tank

Figure 3. Schematic representation of the insulated pipe section during hyperbaric tests

Figure 4. Prototype equipment

Figure 5. Instrumentation of the industrial prototype

Figure 6. Testing programs realized on the prototype - (a) under 1bar pressure (test A), (b) under 300bar hydrostatic pressure (test B)

Figure 7. Boundary conditions and mesh of insulated pipe section for the internal conduction model

Figure 8. Boundary conditions and mesh of insulated pipe section for the internal convection model

Figure 9. Representation of the thermal heat flows during test at 1bar: test A - (a) 120W (step 2), (b) 240W (step 3)

Figure 10. Temperature and displacement distributions within insulated pipe section in the steady state 1bar/120W - Model based on internal conduction

Figure 11. Temperature and displacement distributions within insulated pipe section in the steady state 1bar/120W - Model based on internal convection

Figure 12. Comparison between experimental and simulated temperatures during test at 1bar: test A - (a) 120W (step 2), (b) 240W (step 3)

Figure 13. Comparison between experimental and simulated temperatures during test at 300bar: test B - (a) 120W (step 3), (b) 240W (step 4)

Figure 14. Stress repartition in the syntactic foam - 300bar/240W

Figure 15. Displacements in the radial (r) and vertical (z) directions along the half structure at the internal radius of the syntactic foam

Figure 16. Radial and axial component of the conductive heat flux in the center of the structure

Figure 17. Axial component of the conductive heat flux in the structure obtained with software Comsol

Figure 18. Parametric study about the heat flux repartition: influence of pipe length and thermal conductivity of the material on the radial heat flow percentage

Figure 19. Comparison between experimental and simulated temperatures with transient model during test at 300bar

Figure 20. Influence of the syntactic foam Poisson coefficient value on coating thickness evolution during tests at 120W - (a) 1bar, (b) 300bar